Absolute Configuration of Secondary Alcohols by ^{1}H NMR: In Situ Complexation of α-Methoxyphenylacetic Acid Esters with Barium(II)

Rosa García,[†] José M. Seco,[†] Saulo A. Vázquez,[‡] Emilio Quiñoá,[†] and Ricardo Riguera*[,†]

Departamento de Química Orgánica and Departamento de Química Física, Facultad de Química and Instituto de Acuicultura, Universidad de Santiago de Compostela, E-15782 Santiago de Compostela, Spain

ricardo@usc.es

Received March 8, 2002

A novel methodology that allows the assignment of the absolute configuration of chiral secondary alcohols by NMR using only one derivative is presented. All that is needed is (a) the derivatization of the alcohol of unknown configuration with one enantiomer—either the (*R*)- or the (*S*)—of α-methoxyphenylacetic acid (MPA), (b) the recording of the ^{1}H NMR spectrum of the resulting ester in MeCN-d_3, and (c) addition of a barium(II) salt [i.e. $Ba(ClO_4)_2$] to the NMR tube till saturation and recording of a second spectrum. The assignment of the *R*/*S* configuration to the alcohol takes a few minutes and consists on the comparison of the signs of the shifts ($\Delta\delta^{Ba}$) produced by addition of the barium(II) with those predicted for the (*R*) and the (*S*) enantiomers in accordance to a simplified model that reflects the conformational changes produced by the complexation with barium and their consequences in the chemical shifts. These conformational changes are based on experimental NMR and CD results showing that the formation of a barium(II) complex with the MPA ester moves the conformational equilibrium between *syn*- (sp) and *anti*-periplanar (ap) forms toward the most stable ones (sp), and that this leads to the increase of the shielding caused by the MPA phenyl group on a certain substituent of the alcohol. In addition, ab initio Hartree−Fock (HF) and density functional theory (DFT) calculations provide further evidence on the formation, structure, and stability of the complexes with Ba^{2+}, Mg^{2+}, and the influence of the solvent. The general applicability of this methodology and the reliability of the configurational assignment were assured by the study of about twenty alcohols of known configuration and diverse structural features. Its scope and limitations have also being established and other representative cations (i.e. Li^+, Rb^+, Cs^+, Mg^{2+}, Ca^{2+}, Sc^{3+}, V^{3+}, Zn^{2+}) were also evaluated. The procedure proposed is simple, fast, and cheap because it requires a very small amount of sample, only one derivatization, and the recording of only two ^{1}H NMR spectra at rt. A graphical guide to facilitate the application of this new method is included at the end of the paper.

Introduction

As part of our continuing efforts to establish the use of ^{1}H NMR spectroscopy as a convenient tool for the determination of the absolute stereochemistry of organic compounds in solution, we have in recent years studied the fundamentals of the procedure,[1] proposed new derivatizing reagents and explored their scope and limitations for the study of the stereochemistry of primary[2] and secondary alcohols,[3] primary amines,[4] and carboxylic acids.[5]

In addition to the extension of this method to polyfunctional compounds,[6] a particularly important aim of our research is the optimization and simplification of this approach. In this respect we have improved the method in comparison to previous approaches. For example, in the classical method pioneered by Mosher and Trost,[7] derivatization of the substrate with the two enantiomers of the auxiliary reagent was required. However, we have shown that modulation of the conformational equilibrium in favor of one of the conformers allows a safe assignment of the absolute stereochemistry using only one MPA derivative rather than two.[8]

* To whom correspondence should be addressed.
[†] Departamento de Quimica Organica and Instituto de Acuicultura.
[‡] Departamento de Química Fisica.

(1) (a) Seco, J. M.; Quiñoá, E.; Riguera, R. *Tetrahedron: Asymmetry* **2001**, *12*, 2915−2925. (b) Seco, J. M.; Quiñoá, E.; Riguera, R. *Tetrahedron: Asymmetry* **2000**, *11*, 2781−2791.

(2) (a) Latypov, S. K.; Ferreiro, M. J.; Quiñoá, E.; Riguera, R. *J. Am. Chem. Soc.* **1998**, *120*, 4741−4751. (b) Ferreiro, M. J.; Latypov, S. K.; Quiñoá, E.; Riguera, R. *Tetrahedron: Asymmetry* **1996**, *7*, 2195−2198.

(3) (a) Latypov, S. K.; Seco, J. M.; Quiñoá, E.; Riguera, R. *J. Org. Chem.* **1995**, *60*, 504−515. (b) Seco, J. M.; Latypov, S. K.; Quiñoá, E.; Riguera, R. *Tetrahedron: Asymmetry* **1995**, *6*, 107−110. (c) Seco, J. M.; Quiñoá, E.; Riguera, R. *Tetrahedron* **1997**, *53*, 8541−8564. (d) Latypov, S. K.; Seco, J. M.; Quiñoá, E.; Riguera, R. *J. Org. Chem.* **1996**, *61*, 8569−8577.

(4) (a) Latypov, S. K.; Seco, J. M.; Quiñoá, E.; Riguera, R. *J. Org. Chem.* **1995**, *60*, 1538−1545. (b) Trost, B. M.; Bunt, R. C.; Pulley, S. R. *J. Org. Chem.* **1994**, *59*, 4202−4205. (c) Seco, J. M.; Latypov, S. K.; Quiñoá, E.; Riguera, R. *J. Org. Chem.* **1997**, *62*, 7569−7574. (d) Seco, J. M.; Quiñoá, E.; Riguera, R. *J. Org. Chem.* **1999**, *64*, 4669−4675.

(5) (a) Ferreiro, M. J.; Latypov, S. K.; Quiñoá, E.; Riguera, R. *J. Org. Chem.* **2000**, *65*, 2658−2666. (b) Ferreiro, M. J.; Latypov, S. K.; Quiñoá, E.; Riguera, R. *Tetrahedron: Asymmetry* **1997**, *8*, 1015−1018.

(6) Seco, J. M.; Martino, M.; Quiñoá, E.; Riguera, R. *Organic Lett.* **2000**, *2*, 3261−3264.

(7) (a) Sullivan, G. R.; Dale, J. A.; Mosher, H. S. *J. Org. Chem.* **1973**, *38*, 2143−2147. (b) Trost, B. M.; Bunt, R. C.; Pulley, S. R. *J. Org. Chem.* **1994**, *59*, 4202−4205.

10.1021/jo0256989 CCC: $22.00
Published on Web 05/24/2002

Practical applications of this approach to alcohols[8a,b] and amines[8c] have recently been demonstrated. In the first case, the configurational assignment of a secondary alcohol can be made from only one MPA ester derivative[8b] [either the (*R*)- or the (*S*)-MPA ester of the alcohol] if one compares two NMR spectra acquired at different temperatures. In a completely different approach,[8c] we used selective chelation to shift the conformational equilibrium of an MPA amide in favor of the sp conformer. As a result, we showed that the absolute configuration of an α-chiral primary amine can be determined if one compares the NMR spectra of its MPA amide derivative [either the (*R*)- or the (*S*)-MPA amide] recorded both in the absence and in the presence of a barium salt.

We present here our results on the use of barium(II) complexes for the assignment of the absolute configuration of secondary alcohols by NMR measurements on a single derivative. More specifically, we will report experimental (NMR and CD) and theoretical (ab initio calculations) data that allow the characterization of the conformational changes produced by the addition of barium(II) salts to the NMR tube containing the MPA derivative. The structure of the resulting complex and the stereochemical consequences are subsequently explained. The application of this method to an extensive range of alcohols of varied structure and known absolute stereochemistry is also included in order to demonstrate the general applicability of the method and to define its scope and limitations. A simplified model for the correlation of the spectral data with the absolute configuration of the alcohol is included at the end of the paper.

Results

1. The Addition of a Barium(II) Salt to MPA Esters: NMR and CD Studies. The MPA esters of (−)-menthol are particularly well suited for this study because their conformational composition and the influence of the anisotropic effect of the phenyl group of MPA on the chemical shifts of the substrate have been studied in detail.

In the MPA esters of (−)-menthol, different groups of the alcohol part are under the shielding cone of the phenyl ring in the two main conformers sp and ap. For their part, the C_α-H and MeO groups of the auxiliary MPA are different in each conformer in terms of their orientation with respect to the anisotropic cone of the carbonyl group. Thus, in the (*R*)-MPA ester, Me(8′) and Me(9′) are shielded by the Ph ring in the more stable sp conformer, while Me(10′) is shielded in the less stable conformer ap. In the (*S*)-MPA ester the opposite occurs: Me(10′) is shielded in the more stable conformer sp and Me(8′) and Me(9′) are shielded in the less stable conformer ap (see Figure 1).

A practical consequence of this conformational behavior is that the NMR signals due to Me(8′) and Me(9′) are more shielded by the Ph group in the (*R*)-MPA ester than in the (*S*)-MPA analogue, showing differences of $\Delta\delta^{RS} = -0.207$ and -0.249 ppm, respectively,[9] while the signal due to Me(10′) is more heavily shielded in the (*S*)- than in the (*R*)-MPA ester ($\Delta\delta^{RS} = +0.054$ ppm).

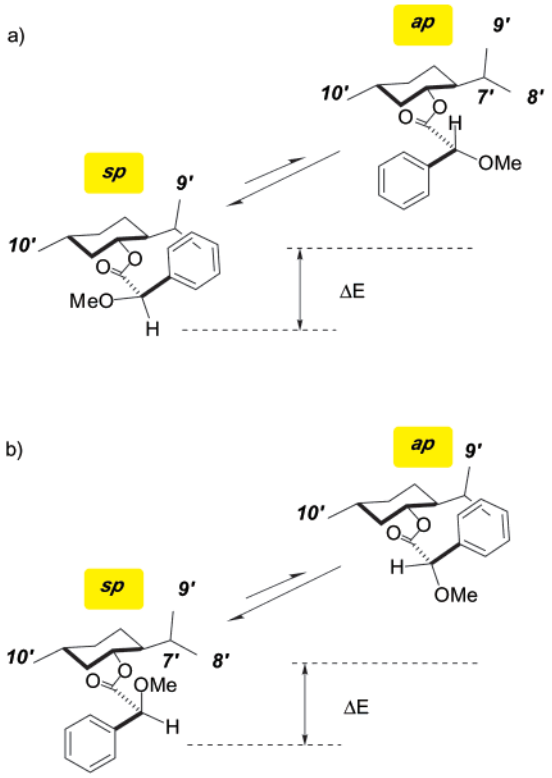

Figure 1. Equilibrium between the two main conformers (*syn*-periplanar and *anti*-periplanar) of the (a) (*R*)-MPA ester of (−)-menthol and (b) the (*S*)-MPA ester.

When the NMR spectra of these MPA esters were recorded using MeCN-d_3 as the solvent and with the solution saturated with barium perchlorate, the following significant changes were observed:

(a) In the (*R*)-MPA ester, the signals due to Me(8′) and Me(9′) were shifted to higher field by $\Delta\delta^{Ba} = +0.132$ and $+0.104$ ppm, respectively,[10] and that of Me(10′) to lower field ($\Delta\delta^{Ba} = -0.017$ ppm), as shown in Figures 2a and 2b.

(b) In the (*S*)-MPA ester, the signal due to Me(10′) shifted to higher field ($\Delta\delta^{Ba} = +0.04$ ppm), while those due to Me(8′) and Me(9′) moved to lower field ($\Delta\delta^{Ba} = -0.025$ and -0.084 ppm, respectively), as shown in Figures 2c and 2d.

(c) In both the (*R*)- and the (*S*)-MPA esters of menthol, the signals due to C_α-H were deshielded [by -0.249 ppm in the (*R*)- and -0.242 ppm in the (*S*)-MPA ester] while those due to the MeO group were shielded [$+0.162$ ppm in the (*R*)- and $+0.100$ ppm in the (*S*)-MPA ester] upon addition of the barium compound.

The behavior described above is practically identical to that previously observed in the low-temperature NMR spectra of the (*R*)- and (*S*)-MPA esters of (−)-menthol[3a] (Table 1) and is related to the redistribution of the sp/ap populations in the equilibrium: at lower temperatures the population of the most stable conformer sp increases in comparison to that of the ap conformer. As a consequence, in the (*R*)-MPA ester the number of molecules (sp) that have the Me(8′) and Me(9′) groups under the

(8) (a) Seco, J. M.; Quiñoá, E.; Riguera, R. *Tetrahedron* **1999**, *55*, 569−584. (b) Latypov, S. K.; Seco, J. M.; Quiñoá, E.; Riguera, R. *J. Am. Chem. Soc.* **1998**, *120*, 877−882. (c) López, B.; Quiñoá, E.; Riguera, R. *J. Am. Chem. Soc.* **1999**, *121*, 9724−9725.

(9) The $\Delta\delta^{RS}$ value for a proton is the difference between its chemical shift in the (*R*)-derivative and its chemical shift in the (*S*)-derivative.

(10) To maintain coherence between the equilibrium shift created upon lowering the temperature and the $\Delta\delta^{T1,T2}$ values, we have defined the $\Delta\delta^{Ba}$ value for a proton as the difference between its chemical shift before the addition of barium(II) and its chemical shift after the addition of barium(II). Note that in the case of amides (ref 8c), $\Delta\delta^{Ba}$ was defined in the opposite way.

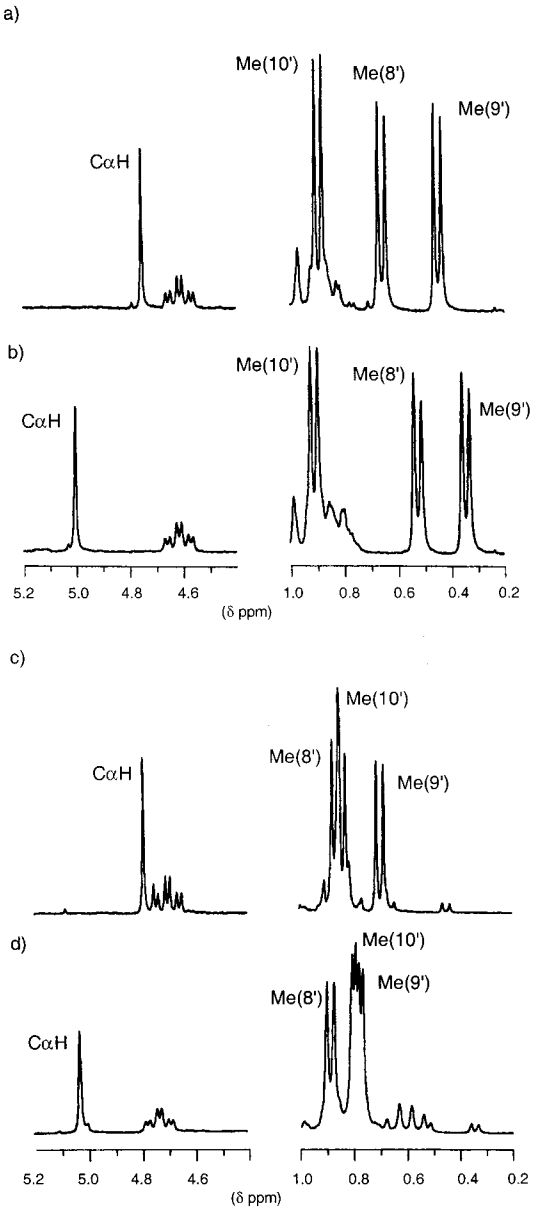

Figure 2. ^{1}H NMR spectrum of (a) the (*R*)-MPA ester of (−)-menthol in MeCN-d_3 (b) upon the addition of a barium(II) salt. ^{1}H NMR spectrum of (c) the (*S*)-MPA ester of (−)-menthol in MeCN-d_3 and (d) upon the addition of a barium(II) salt.

aromatic shielding cone of the Ph group increases and, therefore, their signals become more shielded in the average NMR spectrum. On the other hand, the number of molecules (ap) in which the Me(10′) group is under the aromatic shielding cone diminishes, and therefore the signal for this substituent becomes less shielded in the average spectrum. Similar reasoning applies to the (*S*)-MPA ester.

In summary, when barium(II) ions are added to the appropriate esters, the NMR behavior of these compounds is totally parallel to that observed in the corresponding low-temperature experiments (Table 1): i.e., the protons in question become shielded/deshielded in the same way and intensity in both experiments.

This similarity in the data obtained for the low-temperature experiments and for the addition of Ba^{2+} clearly suggests an identical origin for the effect: the cation provides additional stabilization of the sp conformer, thus shifting the equilibrium to increase the sp population in a similar way to that generated by decreasing the temperature.

Further and independent support for this interpretation was obtained from CD studies. The CD spectra of the (*R*)-MPA and (*S*)-MPA esters of (+)-borneol show a Cotton effect at 226 nm, which is associated with an n−π transition of the carbonyl group. The Cotton effect is not influenced by the chirality of the alcohol and was found to depend on the configuration at the asymmetric center of the auxiliary MPA: it is negative in the (*R*)-MPA esters and positive in the (*S*)-MPA esters. Nevertheless, the octant rule[11] predicts opposite signs and a similar intensity for the sp and ap conformers [negative for the sp and positive for the ap conformer of an (*R*)-MPA derivative; the opposite for the (*S*)-MPA derivatives, Figure 3], and therefore the intensity and sign of this band in the average CD spectrum constitutes a measure of the sp/ap equilibrium.

In fact, the negative Cotton effect observed for the (*R*)-MPA ester of (+)-borneol and the positive CD of the (*S*)-MPA ester originate, in both cases, from the predominance of the sp form (Figure 4).

Given the ability of CD to detect changes in the sp/ap ratio, we decided to use this technique for the study of the conformational changes suggested by the NMR experiments. Indeed, when a series of CD spectra of the (*R*)-MPA ester of (+)-borneol were recorded in the presence of increasing amounts of barium perchlorate, the intensity of the negative band increased, as one would expect if the population of the most stable sp conformer were increased by the presence of the cation (Figure 4).

This increase in the population of the sp conformer shown by both NMR and CD spectroscopy can be completely understood if the Ba^{2+} salt were to form some kind of stabilizing complex with the methoxy and the carbonyl oxygens of the sp conformer, as represented in Figure 5. Indeed, the ability of barium(II) to coordinate with oxygen atoms is well established,[12] and experimental evidence indicating that the carbonyl oxygens are involved in the chelation was obtained from the ^{13}C NMR spectra of the MPA esters of (−)-menthol in the presence of Ba^{2+}. Shifts of −3.55 and −3.36 ppm to lower field for the C=O signals in the (*R*)- and the (*S*)- esters were observed, respectively. Addition of water to the NMR sample breaks up the complex, and the new spectrum is identical to that obtained before the addition of barium.

Further information about this phenomenon was obtained when the changes produced in the NMR spectra by the addition of barium(II) were quantitatively monitored. Known quantities of barium hexafluoropentanodionate salt[13] were added sequentially to the NMR samples containing (*R*)- and (*S*)-MPA esters of (−)-menthol in acetonitrile-d_3 (Figure 6). The expected shifts and regular increase in $\Delta\delta$ were seen (Figure 7). The maximum shift was obtained when a 1:1 molar ratio of

(11) Eliel, E. L.; Wilen, S. H.; Mander, L. N. *Stereochemistry of Organic Compounds*; Wiley-Interscience: New York, 1994.

(12) (a) Shibasaki, M.; Yamada, Y. M. A. *Tetrahedron Lett.* **1998**, *39*, 5561−5564. (b) Rees, W. S.; Caballero, C. R.; Hesse, W. *Angew. Chem., Int. Ed. Engl.* **1992**, *31*, 735−737. (c) Norman, J. A. T.; Pez, G. P. J. *Chem. Soc., Chem. Commun.* **1991**, 971−972. (d) Rees, W. S.; Carris, M. W.; Hesse, W. *Inorg. Chem.* **1991**, *30*, 4481−4484. (e) Ra*β*hofer, W.; Müller, W. M.; Vögtle, F. *Chem. Ber.* **1979**, *112*, 2095−2119.

(13) This barium(II) compound is more soluble in MeCN-d_3 than $Ba(ClO_4)_2$ and is very well suited for titration experiments.

Table 1. Selected Chemical Shifts and Δδ Values for MPA Esters of (−)-Menthol at Two Different Temperatures[a] and in the Absence/Presence[b] of Ba^{2+}

ester	experimental	Me(8′)	Me(9′)	Me(10′)	$C_\alpha H$	MeO
(*R*)-MPA	$T = 296$ K	0.651	0.418	0.888	4.533	3.301
	$T = 153$ K	0.561	0.165	0.898	4.641	3.284
	$\Delta\delta^{T1,T2}$	**+0.090**	**+0.253**	**−0.010**	**−0.108**	**+0.017**
	without Ba^{2+}	0.655	0.446	0.891	4.753	3.512
	with Ba^{2+}	0.523	0.342	0.908	5.002	3.350
	$\Delta\delta^{Ba}$	**+0.132**	**+0.104**	**−0.017**	**−0.249**	**+0.162**
(*S*)-MPA	$T = 296$ K	0.846	0.642	0.822	4.567	3.307
	$T = 153$ K	0.895	0.681	0.785	4.636	3.257
	$\Delta\delta^{T1,T2}$	**−0.049**	**−0.039**	**+0.037**	**−0.069**	**+0.050**
	without Ba^{2+}	0.862	0.695	0.837	4.782	3.357
	with Ba^{2+}	0.887	0.779	0.797	5.024	3.257
	$\Delta\delta^{Ba}$	**−0.025**	**−0.084**	**+0.040**	**−0.242**	**+0.100**

[a] In CS_2:CD_2Cl_2 (4:1). [b] In MeCN-d_3.

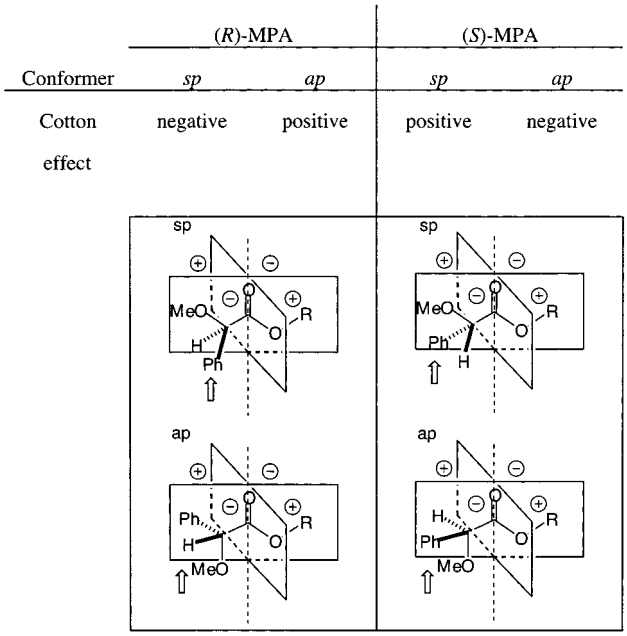

Figure 3. Cotton effects for the main conformers of MPA derivatives and octant rules. The sign of the Cotton effect is defined by the quadrant occupied by the phenyl group.

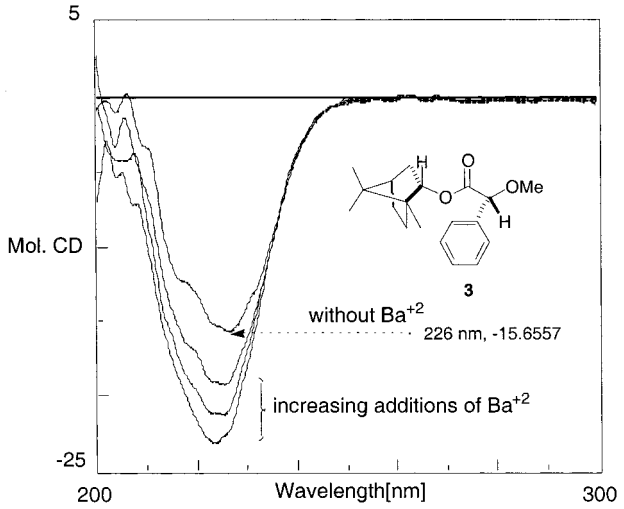

Figure 4. CD spectrum of the (*R*)-MPA ester of (+)-borneol (**3**) in the presence of increasing amounts of Ba^{2+} [$c = 1.10-3$ M of **3**, $v = 300$ μL, MeCN, sequential additions of 10 mg of $Ba(ClO_4)_2$].

barium(II)/ester was used, and further addition of barium did not produce any significant changes,[14] showing that the stoichiometry of the complex is 1:1.

In an effort to ascertain whether addition of salts other than Ba^{2+} could produce similar shifts, we examined the NMR spectra of some MPA esters in the presence of different amounts of $LiClO_4$, $RbClO_4$, CsI, $Mg(ClO_4)_2$, $CaCO_3$, $Sc(OTf)_3$, $(acac)_3V$, $(acac)_2VO$, ZnI_2. Overall, we found that the shifts obtained in these experiments were either too small to be of use, could not be attributed to a particular identifiable complex, or did not correspond to any discernible pattern.

This situation was the same even on using divalent cations, such as Ca^{2+} and Mg^{2+}, that are well-known for their ability to coordinate with oxygen donors. Figure 8 illustrates this situation in terms of the Δδ data obtained after addition of Mg^{2+} to the esters of alcohols **3** and **17** (previously shown to behave like the esters of menthol (**1**) in the presence of Ba^{2+}; see Figure 10). As can be observed, the signals for some protons (underlined values) move in the presence of the metal in the sense opposite to that expected, thus leading to an irregular Δδ sign distribution.

Theoretical calculations concerning the stability and conformation of the MPA esters and their complexes, as well as the role of the solvent, helped to provide an explanation for this behavior based on solvent effects.

Finally, it is important to point out that other experimental techniques, such as MS, also provided further evidence substantiating the formation of the barium(II) complexes. For instance, the FAB−(+) of the (*S*)-MPA ester of compound **14** (Figure 10) in MNBA and in the presence of $Ba(ClO_4)_2$ generated a strong base peak at $m/z = 627$ corresponding to a [**14** + Ba + ClO_4]$^+$ species

2. Theoretical Calculations. To assess the reliability of the explanations put forward to justify the NMR and CD results, we decided to carry out theoretical studies [ab initio Hartree−Fock (HF) and density functional theory (DFT) calculations—see detailed information in the Experimental Section] on the formation, structure, and stability of the conformers of the (*R*)-MPA ester of 2-propanol (used as a model compound), their complexes with Ba^{2+} and Mg^{2+}, and the influence of the solvent.

The results of the theoretical studies into the structure and stability of the conformers of the (*R*)-MPA ester are shown in Figure 9a and Table 2. The most relevant conformers are presented in Figure 9a and their relative

(14) The molar ratio was measured by integration of the olefinic proton of the hexafluoropentanodionate ($\delta = 5.79$) with respect to the $C_\alpha H$ proton of the MPA ester.

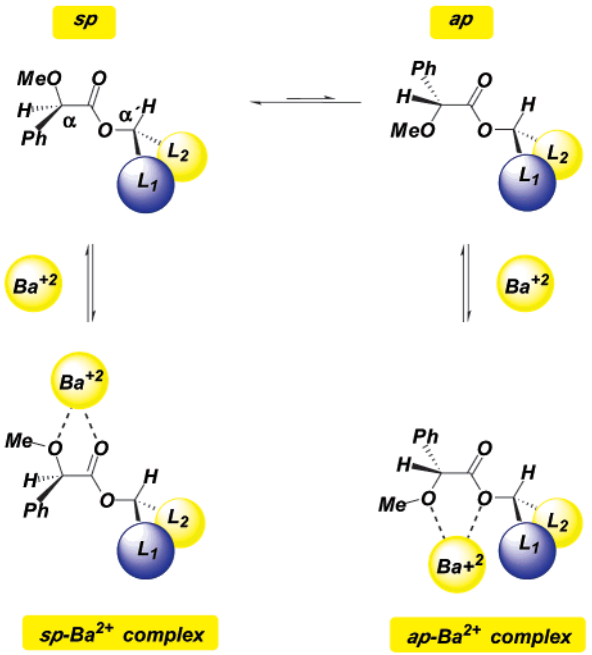

Figure 5. Formation of Ba^{2+} complexes for MPA esters.

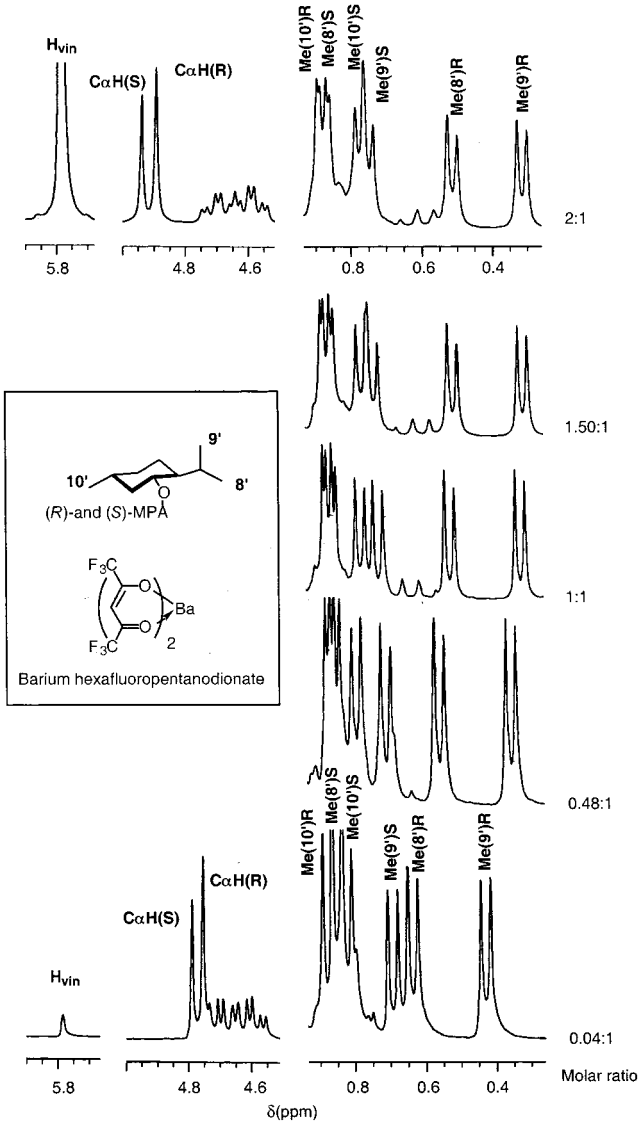

Figure 6. Evolution of the ^{1}H NMR spectra of the (*R*)- and (*S*)-MPA esters of (−)-menthol upon sequential additions of barium hexafluoropentanodionate in MeCN-d_3.

energies, and the values for the (Me)O−C_α−C═O and Me−O−C_α−C(═O) dihedral angles, in Table 2. The results confirm our previous studies[3] on the existence of two major types of conformers in equilibrium (*syn*-periplanar or sp and *anti*-periplanar or ap) for MPA esters defined by the relative position of the MeO and C═O groups (Figures 1 and 5). In fact, these calculations produce two sp forms (sp1 and sp2) and two ap forms (ap1 and ap2) that differ in the position of the Me−O bond.[15] The sp conformers are the most populated. As the Ph group in sp1 and sp2 occupies the same relative position with respect to L_1/L_2, both conformations are equivalent from the NMR point of view, and the same occurs with ap1 and ap2.

At the HF/LanL2DZ level of theory, the most stable conformation in the gas phase has a *syn*-periplanar (sp*1*) (Me)O−C_α−C═O arrangement (15.6°), with the other *syn*-periplanar form [sp*2*, (Me)O−C_α−C═O = 39.2°] being 1.1 kcal/mol less stable than sp1.[16] The two *anti*-periplanar conformations (ap1 and ap2) are slightly higher in energy (0.5 and 0.8 kcal/mol, respectively). The more accurate B3LYP method also predicts sp1 to be the most stable conformation, although the relative energies for the other conformations, which differ slightly from the HF values, are within 1 kcal/mol. The most significant change occurs for sp2, where the relative energy decreases by 0.5 kcal/mol.

When solvent effects were taken into account by using the Onsager model,[17,18] we found that the relative energies of the above conformations do not vary substantially: the changes are within 0.5 kcal/mol. Likewise, the geometries do not undergo considerable changes on going from the gas phase to solution. The most relevant change concerns the (Me)O−C_α−C═O dihedral angle in the sp2 conformation (39.2° in the gas phase vs 34.6° in solution). The geometries optimized with the Onsager model were then used to obtain more accurate energies by employing the IEFPCM[19] and IPCM[20] models, in both cases through single-point B3LYP/LanL2DZ calculations. The relative energies calculated by IEFPCM are rather similar to the gas-phase energies determined by DFT. The two syn conformations (sp1 and sp2) are now found to be isoenergetic and somewhat more stable (∼1 kcal mol^{-1}) than

(15) The two components of each sp1/sp2 and ap1/ap2 pair differ mainly in the orientation of the Me−O−C_α−C(═O) arrangement, which is gauche for sp1/ap2 and anti for sp2/ap1.

(16) In all the conformations studied here, the $C_{\alpha'}$−O−C═O skeletal fragment was considered in its most stable orientation: i.e., the *Z* conformation. In keeping with the notation used in our previous publications, we use the (Me)O−C_α−C═O torsion angle to denote the conformations optimized in this study: *syn*-periplanar (sp) and *anti*-periplanar (ap). Conformer sp*2* can also be considered as *syn*-clinal (sc) and the conformers ap1 and ap2 as *anti*-clinal if the classification of torsion angles proposed by Klyne and Prelog are used instead. See: Klyne, W.; Prelog, V. *Experientia* **1960**, *16*, 521−523.

(17) Onsanger, L. *J. Am. Chem Soc.* **1936**, *58*, 1486−1493.

(18) (a) Wong, M. W.; Wiberg, K. B.; Frisch, M. J. *J. Chem. Phys.* **1991**, *95*, 8991−8898. (b) Wong, M. W.; Frisch, M. J.; Wiberg, K. B. *J. Am. Chem. Soc.* **1991**, *113*, 4776−4782.

(19) (a) Tomasi, J.; Mennucci, B.; Cancès, E. *J. Mol. Struct. (THEOCHEM)* **1999**, *462*, 211−226. (b) Cossi, M.; Barone, V.; Mennucci, B.; Tomasi, J. *Chem. Phys. Lett.* **1998**, *286*, 253−260. (c) Cancès, E.; Mennucci, B.; Tomasi, J. *J. Chem. Phys.* **1997**, *107*, 3032−3041.

(20) Foresman, J. B.; Keith, T. A.; Wiberg, K. B.; Snoonian, J.; Frisch, M. J. *J. Phys. Chem.* **1996**, *100*, 16098−16104.

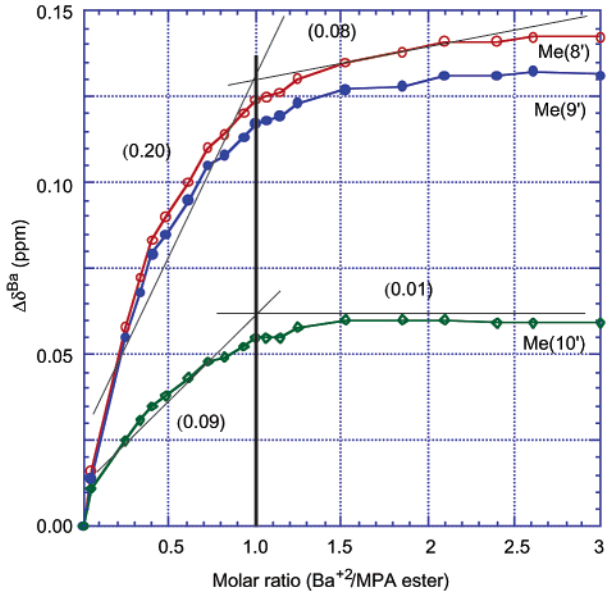

Figure 7. Evolution of $\Delta\delta^{Ba}$ magnitudes (in ppm) for Me(8′), Me(9′) [in the (*R*)-MPA ester], and Me(10′) [in the (*S*)-MPA ester] of (−)-menthol upon increasing additions of barium(II). Slopes are shown in parentheses.

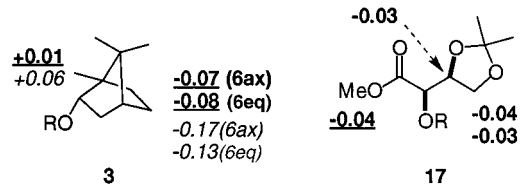

Figure 8. Selected $\Delta\delta^{Mg}$ values (ppm in MeCN-d_3) for (*R*)- (in bold) and (*S*)- (in italic) MPA esters of the substrates shown upon addition of $Mg(ClO_4)_2$. The values underlined do not show the expected sign.

the anti conformations (ap1 and ap2). The IPCM energies, however, differ significantly from the others. The sp2 conformation is predicted to be the most stable by 2−3 kcal mol^{-1}, on considering the conformations studied here, and ap1 is predicted to be a little more stable than sp1. In addition, the IPCM results show a clear preference for the *anti*-periplanar orientation of the Me-O−C_α−C(=O) arrangement. Overall, the calculations suggest that syn and anti conformations coexist in acetonitrile at room temperature, with the syn population (sp1 + sp2) being larger that the anti.

Once the MPA ester equilibrium had been elucidated, the complexes with Ba^{2+} and Mg^{2+} were submitted to an analogous study. The results of these calculations are given in Table 3. Unfortunately, in several cases the calculations including solvent effects showed convergence problems. Therefore, we present only the gas-phase results. Two different conformations were optimized: sp-M^{2+} and ap-M^{2+}. In sp-M^{2+}, the divalent cations form the complex between the methoxy and the carbonyl oxygens, while in ap-M^{2+} the oxygens involved are those of the methoxy and alkoxy groups (*not* the carbonyl, see Figure 9b). The gas-phase calculations show a clear preference for the sp-M^{2+} conformation. In the case of Ba^{2+}, the ap-Ba^{2+} conformation is 13.9 kcal/mol higher in energy at the HF level and 10.1 kcal/mol higher at the B3LYP level. For Mg^{2+}, the corresponding values are somewhat lower at 10.9 and 7.0 kcal/mol, respectively. The calculations also show that complexation modifies the spatial orientation of the phenyl group in the ap conformer, with the ring plane adopting a perpendicular disposition with respect to the C_α−H bond as opposed to the usual coplanar or almost coplanar arrangement. A consequence of this turn is that the aromatic ring in now in a less favorable position to project its anisotropic effect on the substituents L_1 and L_2. This fact, together with the smaller population, explains why the anisotropic effect of the phenyl group on L_1/L_2 is less relevant in the ap-M^{2+} forms than in the sp-M^{2+} conformers (favorable orientation of the phenyl ring and higher population).

Finally, we analyzed the interactions of Ba^{2+} and Mg^{2+} ion with the solvent (acetonitrile). Using the supermolecule method[21] and considering an octahedral arrangement of acetonitrile molecules around the cation, the ion−solvent interaction energies at the B3LYP//HF level (B3LYP single-point calculations at the HF optimized geometries) were computed to be 237 kcal/mol for Ba^{2+} and 397 kcal/mol for Mg^{2+}. These data follow the expected trend in that the ion−solvent interaction energy increases substantially as the size of the ion decreases[22] and provide a satisfactory explanation for the experimental fact that magnesium(II) cations, or similar ions, do not generate a single and identifiable complex [unlike barium(II)]. This situation arises because the solvation is so strong that it interferes with the formation of the complex with the substrate, and consequently the signal shifts obtained cannot be easily correlated to the structure of the substrate.

In conclusion, these theoretical studies corroborate the hypothesis that the role of barium(II) is to shift the equilibrium by preferential chelation with the sp-M^{2+} form through the methoxy and carbonyl oxygen atoms. In addition, the calculated solvent−cation interactions explain why other metals that are known to complex with oxygen donors are not appropriate for this method. The calculated values also illustrate the delicate balance leading to the MeCN/Ba^{2+} system, which is the most suitable for our NMR studies.

3. Application to the Assignment of Absolute Configuration of Chiral Secondary Alcohols: Scope and Limitations. To test the general applicability of the chelation process, its scope, limitations and consequences, the NMR spectra of a series of secondary alcohols of known absolute stereochemistry and varied structures and substituents were studied in the presence of Ba^{2+}. The (*R*)- and (*S*)-MPA esters of these alcohols were prepared and the NMR spectra recorded in MeCN-d_3 both before and after saturation with dry, finely powdered barium perchlorate. Figure 10 shows the structures of the compounds along with the displacements of the signals produced upon saturation with barium perchlorate measured as $\Delta\delta^{Ba}$. The signs of these shifts[10] are perfectly coherent with the selective formation of the barium(II) chelate with the sp conformer and the corresponding increase in its population. In all cases, substituents from the alcohol that are situated on one side of the plane defined by (Me)OCαC(O)OCα′H (Figure 5) move to higher field upon addition of barium, while those on the other side of the plane shift to lower field. This

(21) (a) Hobza, P.; Zaradník, R. *Intermolecular Complexes*; Elsevier: Amsterdam, 1988. (b) van Duijneveldt-van de Rijdt, J. G. C. M.; van Duijneveldt, F. B.; van Lenthe, J. H. *Chem. Rev.* **1994**, *94*, 1873−1885.

(22) Cabaleiro-Lago, E.; Ríos, M. A. *Chem. Phys.* **2000**, *254*, 11−23.

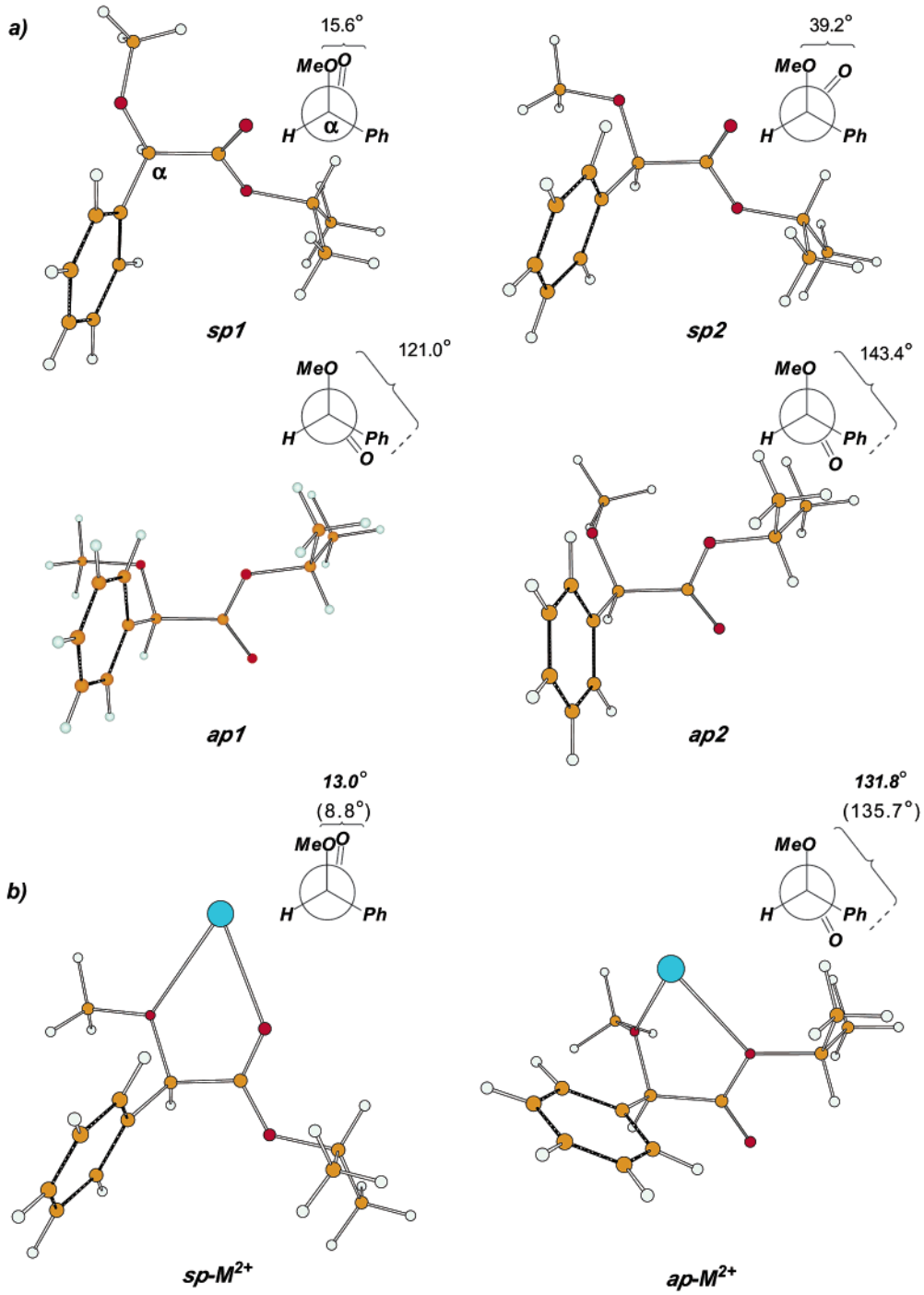

Figure 9. (a) Conformers of the (*R*)-MPA ester of 2-propanol cited in Table 2. Newman projections show the (Me)O−Cα−C═O torsion angles (HF optimized geometries). (b) Conformers of the M^{2+} (Ba^{2+} and Mg^{2+}) complexes of the same ester cited in Table 3. Torsion angles are for the Ba^{2+} (bold) and Mg^{2+} (parentheses) complexes.

situation is reflected in the regular distribution of the signs of $\Delta\delta^{Ba}$, which are positive for one side and negative for the other. As mentioned earlier, the pattern of sign distribution for an MPA ester is essentially identical to that observed when two spectra of the same ester are taken at two different temperatures.

In fact, if a molecular model of the sp conformer of one of the MPA esters is considered, the signal due to the substituent on the alcohol that is in front of the Ph group (i.e. L_1 in Figure 5) shifts to higher field upon addition of barium(II) (positive $\Delta\delta^{Ba}$) while the signal for substituent L_2, which is directed away from the Ph ring in the sp conformer, moves to lower field (negative $\Delta\delta^{Ba}$).

From a practical point of view, these results are extraordinarily important because they indicate that chelation shifts and $\Delta\delta^{Ba}$ signs can be used to correlate the spatial location of the Ph group of the auxiliary MPA (absolute configuration of the auxiliary) with the spatial location of the substituents L_1/L_2 of the alcohol (absolute configuration of the alcohol). Moreover, this correlation can be made using only one derivative [either the (*R*)- or the (*S*)-MPA ester], and it holds for a wide variety of secondary alcohols.

The application of this method is illustrated in Figure 11, which shows the changes observed in the spectra of the (*R*)-MPA ester of diacetone D-glucose after addition

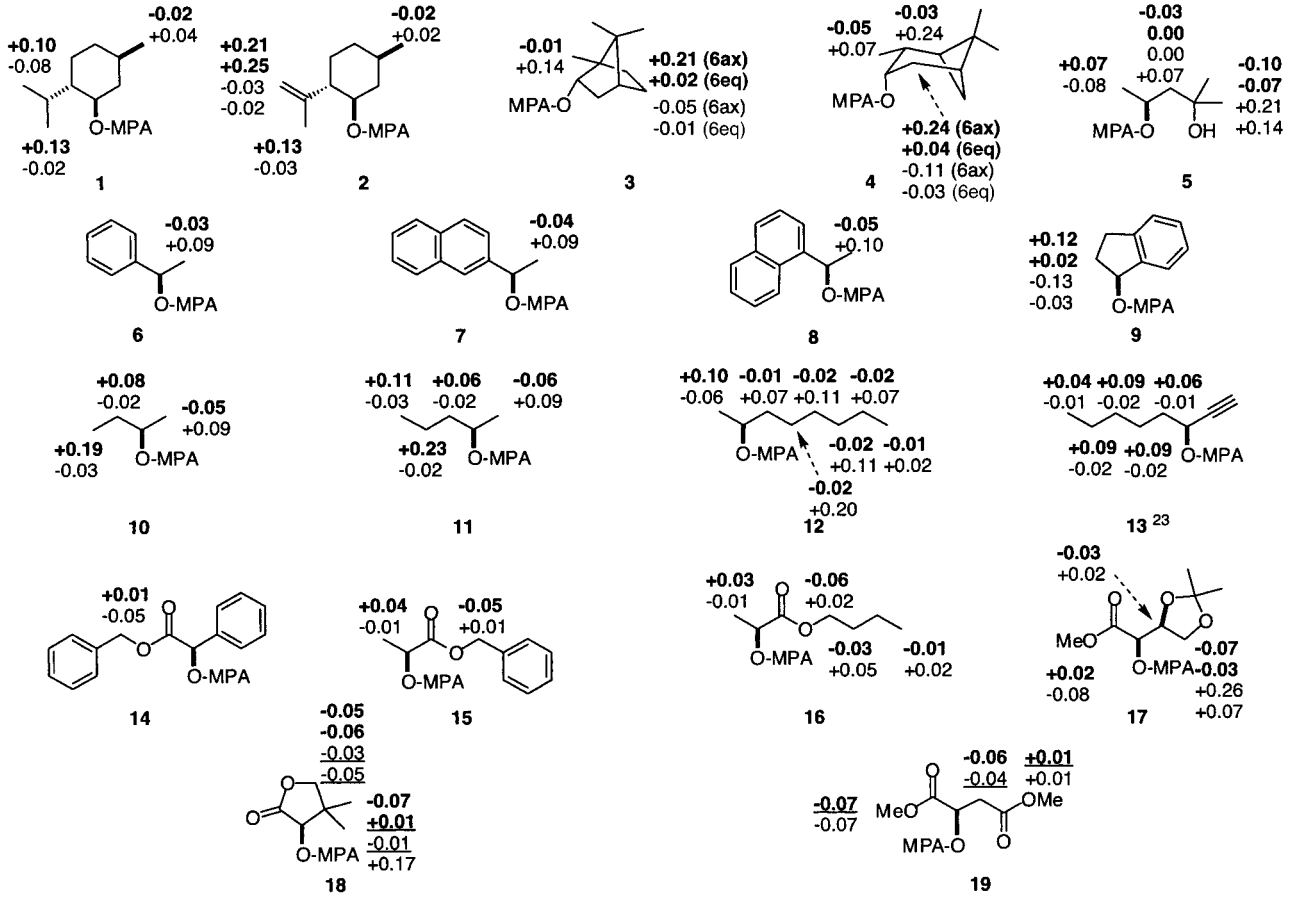

Figure 10. Selected $\Delta\delta^{Ba}$ values (ppm) obtained from the ^{1}H NMR spectra of the (*R*)- (in bold) and (*S*)- (in italic) MPA esters of structurally representative chiral esters.

Table 2. (a) Relative Energies[a] (in kcal/mol), (b) Relative Populations,[b] and (c and d) Relevant Torsion Angles[c] (in degrees) for the Conformations of the MPA Ester of 2-Propanol

			HF	B3LYP/HF[d]	Onsager	IEFPCM[e]	IPCM[f]
sp	sp1	a	**0.0**	**0.0**	**0.0**	**0.0**	**2.6**
		b	*1.00*	*1.00*	*1.00*	*1.00*	*0.01*
		c	15.6°		17.0°		
		d	68.6°		68.8°		
	sp2	a	**1.1**	**0.5**	**0.8**	**0.0**	**0.0**
		b	*0.16*	*0.43*	*0.30*	*1.00*	*1.00*
		c	39.2°		34.6°		
		d	167.6°		167.0°		
ap	ap1	a	**0.5**	**0.7**	**0.9**	**1.0**	**1.9**
		b	*0.43*	*0.31*	*0.22*	*0.18*	*0.04*
		c	121.0°		119.9°		
		d	−161.5°		−163.5°		
	ap2	a	**0.8**	**0.5**	**1.3**	**0.8**	**3.0**
		b	*0.30*	*0.43*	*0.11*	*0.30*	*0.006*
		c	143.4°		145.1°		
		d	−66.2°		−65.5°		

[a] Values in black. All the calculations were performed with the LanL2DZ basis set. [b] Values in italic. Calculated from the Boltzmann distribution at 298.15 K. [c] Entries c correspond to the (Me)O−C_α−C=O torsion angles and entries d to the Me-O−C_α−C(=O) ones. [d] Single-point calculations at the HF optimized geometries. [e] IEFPCM energies calculated with B3LYP and based on Onsager model HF geometries. [f] IPCM energies calculated with B3LYP and based on Onsager model HF geometries.

Table 3. (a) Relative Energies[a] (in kcal/mol) and (b and c) Relevant Torsion Angles[b] (in degrees) for the Most Relevant Conformations of the Complexes of the MPA Ester of 2-Propanol with Ba^{2+} and Mg^{2+}

		HF	B3LYP//HF[c]
sp-Ba^{2+}	a	**0.0**	**0.0**
	b	13.0°	
	c	169.5°	
ap-Ba^{2+}	a	**13.9**	**10.1**
	b	131.8°	
	c	−100.1°	
sp-Mg^{2+}	a	**0.0**	**0.0**
	b	8.8°	
	c	172.7°	
ap-Mg^{2+}	a	**10.9**	**7.0**
	b	135.7°	
	c	−111.2°	

[a] Values in black. All the calculations were performed with the LanL2DZ basis set. [b] Entries b correspond to the (Me)O−C_α−C=O torsion angles and entries c to the Me−O−C_α−C(=O) ones. [c] Single-point calculations at the HF optimized geometries.

of barium(II) perchlorate: protons H(4′), H(5′), H(6′), which are on one side of the chiral center, are shielded by the Ph group in the sp conformer. Upon the addition of barium(II), the sp population increases and those protons are further shielded. Protons H(1′), H(2′), which are on the other side, are shielded by the Ph group in the ap form. The population of this form decreases when barium(II) is added and protons H(1′), H(2′) are deshielded. Interpretation of these shifts according to the chelation model implies the configuration shown for C(3′), which is in perfect agreement with the experimental facts.

Naturally, as these shifts are based on the selective formation of the chelate in the MPA part of the molecule, the presence in the substrate of functional groups that could form other competing complexes with barium may disturb the conformational equilibrium and produce

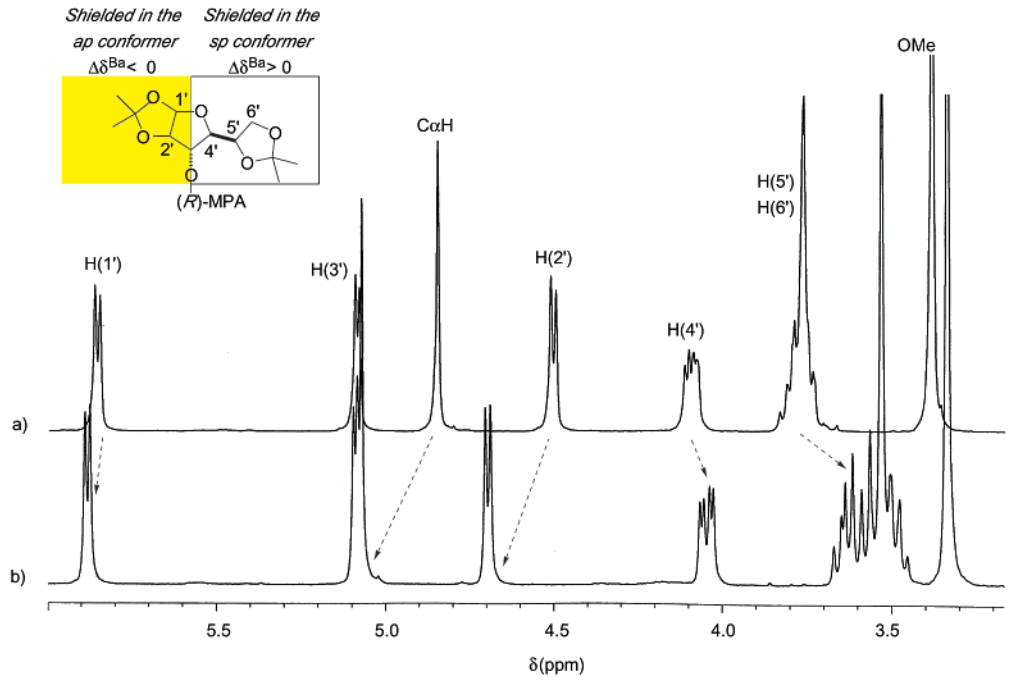

Figure 11. Partial ^{1}H NMR spectra (250 MHz) for the (*R*)-MPA ester of diacetone D-glucose (a) before and (b) after the addition of Ba^{2+}.

unexpected shifts in some protons. There are plenty of examples of barium complexes in the literature, mainly involving oxygen and nitrogen donors such as diketonates and α-alkoxycarbonyls.[12]

To evaluate the importance of this potential limitation we analyzed the NMR behavior of several secondary alcohols bearing extra carbonyl (ester) groups (compounds **14**−**19**). We found that while compounds **14**−**17** (Figure 10) do show the expected distribution for the signs of $\Delta\delta^{Ba}$, alcohols **18** and **19** lead to irregularities in the signs for some protons (underlined data), probably due to some disturbance of the conformational equilibrium caused by additional chelation.

As mentioned previously, the search for other metal cations able to produce selective shifts similar to those described above indicated that barium(II) is the best choice. Other combinations of salts (i.e. $BaCl_2$) and solvents were also tested and these did not offer any advantage over the $Ba(ClO_4)_2$/MeCN-d_3 and hexafluoropentanodionate/MeCN-d_3 systems. Both of these systems generate similar results, and so the former, due to its lower cost, can be recommended in most cases. The standard procedure for the use of this system consists of the addition of powdered, dried $Ba(ClO_4)_2$ directly to the NMR tube containing the ester in MeCN-d_3 until saturation is achieved.

As a guide to the reader interested in the use of Ba^{2+} chelation shifts for the assignment of the absolute configuration of a secondary alcohol, we present a stepwise summary of the procedure in Figure 12. The sample of unknown configuration is reacted with the (*R*)- or the (*S*)-MPA reagent, the spectrum of the resulting MPA ester is recorded in MeCN-d_3, and the signals of L_1 and L_2 are assigned. A second spectrum is recorded after solid anhydrous $Ba(ClO_4)_2$ is added to the NMR tube until saturation, and the chemical shifts signals of L_1 and L_2 are assigned. Then, the $\Delta\delta^{Ba}$ values are calculated. The models shown in Figure 12 are used to place L_1 and L_2 in space in accordance with the signs of $\Delta\delta^{Ba}$.

Conclusion

In conclusion, we have shown that the absolute configuration of a secondary alcohol can be assigned by analysis of the changes produced upon addition of a barium salt in the NMR spectra of the MPA ester [either the (*R*) or the (*S*) enantiomer] derivative. Numerous alcohols of known absolute configuration have been studied in order to demonstrate the general applicability of this method and to evaluate its scope and limitations. The presence of additional chelating functional groups in the alcohol structure and the potential use of other metals have also been assessed.

High-level theoretical calculations and experimental data indicate that the origin of this phenomenon is the preferential chelation with Ba^{2+} of one of the conformers of the MPA esters. The resulting change in the conformational equilibrium is transmitted via aromatic shielding effect to the NMR spectra, where changes in chemical shifts of signals are measured as $\Delta\delta^{Ba}$ values.

The procedure presented is simple, fast and cheap, it requires a very small amount of sample, only one derivatization, and the recording of just two ^{1}H NMR spectra taken at rt.

A simplified graphical model is presented that allows the direct assignment of the absolute configuration of the alcohol from the NMR spectra of the MPA ester.

Experimental Section

Computational Methods. Ab initio Hartree−Fock (HF) and density functional theory (DFT) calculations were performed to elucidate the conformational preferences of the (*R*)-MPA ester of 2-propanol, taken as a model compound, as well as its complexes with Ba^{2+} and Mg^{2+}. We used the standard LanL2DZ basis set, which consists of the Dunning/Huzinaga full double-ζ (D95)[24] for the first row, and Los Alamos effective

(23) The shifts generated by the methine proton of an acetylenic group, such as in compound **13** cannot be trusted for assignment purposes: see ref 8b.

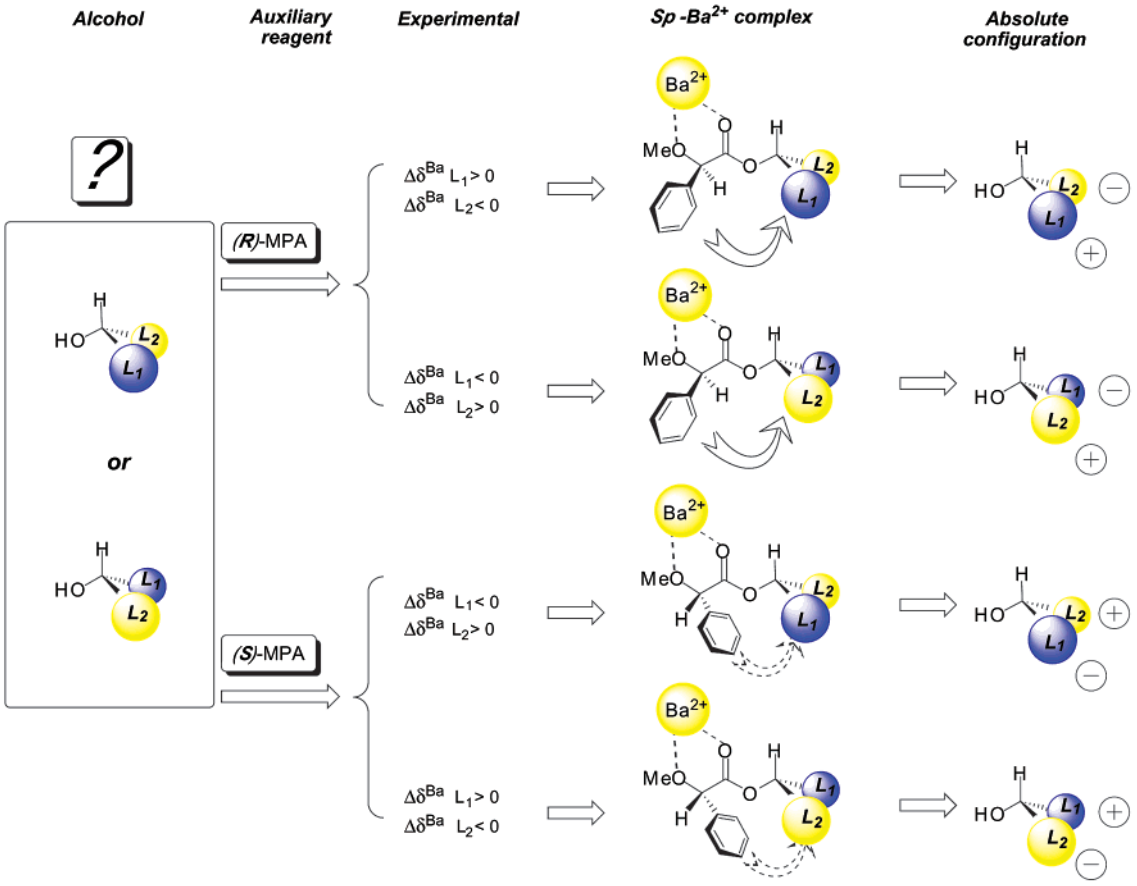

Figure 12. Diagram to deduce the absolute configuration of a chiral secondary alcohol from the $\Delta\delta^{Ba}$ experimental values of either the (*R*)- or the (*S*)-MPA ester.

core potentials plus double-ζ functions on Na−Bi.[25−27] The geometries of the most relevant conformations of the MPA ester, selected from our previous work,[3] were first optimized at the HF/LanL2DZ level. Because of the size of the system, the calculations were restricted to conformations with the $C_{\alpha'}$−O−C=O skeletal fragment in its most stable orientation: i.e., the *Z* conformation. For the determination of more accurate energies, single-point calculations at the HF optimized geometries were carried out using the DFT/B3LYP approach. This method combines Becke's three-parameter nonlocal hybrid exchange potential[28] with the nonlocal correlation functional of Lee, Yang, and Parr.[29] This formalism has been found to be very reliable as far as the description of ion−molecule complexes is concerned.[30]

For the MPA ester, solvent effects were considered using three continuum models: the Onsager model,[17,18] the polarizable continuum model using the integral equation formalism (IEFPCM),[19] and the isodensity surface-polarized continuum model (IPCM).[20] The Onsager model considers a polarizable reference molecule as being in a spherical vacuum cavity. The surroundings of the molecule are treated as a continuum with the macroscopic dielectric constant of the solvent (ϵ = 36.64 for acetonitrile at room temperature). The reference molecule is treated as a point dipole placed in the center of the cavity. A dipole in the molecule will induce a dipole in the medium, and the electric field applied by the solvent dipole will in turn interact with the molecular dipole, leading to net stabilization. With this model, full geometry optimizations were performed starting from the corresponding gas-phase geometries and using the self-consistent reaction field method.[18] The polarizable continuum model (PCM) considers a charge distribution of the solute represented by a discrete number of point charges placed at the centers of the cavity surface elements of the appropriate area, which consist of interlocking spheres. This model also includes nonelectrostatic contributions, namely cavitation, dispersion, and repulsion energies. In the IEFPCM model,[19] the PCM calculation is performed using the integral equation formalism model. The IPCM model[20] defines the cavity as an isodensity surface of the molecule. The surface potential is calculated, and its interaction with the solvent computed self-consistently. The IEFPCM and IPCM energies were obtained by single-point B3LYP/LanL2DZ calculations over the Onsager model optimized geometries. Attempts were made to calculate the conformational energies for the complexes of Ba^{2+} and Mg^{2+} using solvation models, but in several cases success was not achieved.

The interaction energies for Ba^{2+} and Mg^{2+} in acetonitrile were also calculated. This ion−solvent interaction energy was estimated by the supermolecule method,[21] considering $M(CH_3CN)_6$ (with M = Ba^{2+} or Mg^{2+}) octahedral clusters. All the calculations were performed with the Gaussian94 and Gaussian98 series of programs.[31]

General. (*R*)- and (*S*)-MPA (auxiliary reagents) and chiral secondary alcohols are commercially available. MPA esters were prepared according to published procedures. ^{1}H NMR (250 and 300 MHz) and ^{13}C NMR (75.42 MHz). Chemical shifts

(24) Dunning, T. H., Jr.; Hay, P. J. In *Modern Theoretical Chemistry*; Schaefer, H. F., Ed.; Plenum: New York, 1976; Vol. 3, p 1.
(25) Hay, P. J.; Wadt, W. R. *J. Chem. Phys.* **1985**, *82*, 270−283.
(26) Wadt, W. R.; Hay, P. J. *J. Chem. Phys.* **1985**, *82*, 284−298.
(27) Hay, P. J.; Wadt, W. R. *J. Chem. Phys.* **1985**, *82*, 299−310.
(28) (a) Becke, A. D. *J. Chem. Phys.* **1993**, *98*, 5648−5652. (b) Becke, A. D. *J. Chem. Phys.* **1992**, *96*, 2155−2160.
(29) Lee, C.; Yang, W.; Parr, R. G. *Phys. Rev.* **1988**, *B37*, 785−789.
(30) (a) Luna, A.; Amekraz, B.; Tortajada, J. *Chem. Phys. Lett.* **1997**, *266*, 31−37. (b) Hoyau, S.; Ohanessian, G. *Chem. Phys. Lett.* **1997**, *280*, 266−272. (c) Luna, A.; Amekraz, B.; Morizur, J.-P.; Tortajada, J.; Mó, O.; Yáñez, M. *J. Phys. Chem.* **1997**, *101*, 5931−5941. (d) Luna, A.; Amekraz, B.; Tortajada, J.; Morizur, J.-P.; Alcamí, M.; Mó, O.; Yáñez, M. *J. Am. Chem. Soc.* **1998**, *120*, 5411−5426. (e) Kemper, P. R.; Weis, P.; Bowers, M. T.; Maitre, P. *J. Am. Chem. Soc.* **1998**, *120*, 13494−1350.

(δ) are given in ppm relative to TMS in MeCN-d_3. CD studies (200−300 nm, MeCN) were performed in 300 μL cells at concentrations of ester substrates of $1 \cdot 10^{-3}$ M.

General Procedure for Configuration Assignment. The alcohol is reacted with the (*R*)- or the (*S*)-MPA reagent,[3] the spectrum of the resulting MPA ester is recorded in MeCN-d_3 (i.e. 5 mg of ester in 0.5 mL of MeCN-d_3), and the signals of L_1 and L_2 are assigned. Solid anhydrous $Ba(ClO_4)_2$ is added to the NMR tube until saturation is attained (about 200 mg per tube) and a new spectrum recorded. The signals are assigned, and the $\Delta\delta^{Ba}$ value is calculated. The models shown in Figure 12 are used to place L_1 and L_2 in space in accordance with the signs of $\Delta\delta^{Ba}$.

Spectroscopic Data for New Compounds. (*S*)-4-Methyl-4-ol-pentan-2-yl (R)-α-methoxy-α-phenylacetate [(*R*)-5]: $[\alpha]_D = +107.43$ ($c = 0.015$; $CHCl_3$); ^{1}H NMR (250.17 MHz, MeCN-d_3) δ (ppm) 1.06 (d, $J = 6.30$ Hz, 3H), 1.08 (s, 6H), 1.59 (dd, $J = 3.50$, 14.90 Hz, 1H), 1.77 (dd, $J = 8.0$, 14.90 Hz, 1H), 2.50 (s, 1H), 3.35 (s, 3H), 4.76 (s, 1H), 5.14 (m, 1H), 7.33−7.41 (m, 5H); ^{13}C NMR (75.42 MHz, MeCN-d_3), δ 20.3, 28.1, 29.4, 48.1, 56.4, 68.6, 68.9, 82.1, 126.8, 128.1, 136.5, 169.9; MS (EI) *m*/*z* % 266 (M^+).

(*S*)-4-Methyl-4-ol-pentan-2-yl (*S*)-α-methoxy-α-phenylacetate [(*S*)-5]: $[\alpha]_D = -41.27$ ($c = 0.021$; $CHCl_3$); ^{1}H NMR (250.17 MHz, MeCN-d_3) δ (ppm) 0.85 (s, 3H), 0.95 (s, 3H), 1.21 (d, $J = 6.30$ Hz, 3H), 1.55 (dd, $J = 3.60$, 14.80 Hz, 1H), 1.69 (dd, $J = 8.00$, 14.90 Hz, 1H), 2.33 (s, 1H), 3.33 (s, 3H), 4.73 (s, 1H), 5.06 (m, 1H), 7.33−7.58 (m, 5H); ^{13}C NMR (75.42 MHz, MeCN-d_3) δ 20.7, 27.8, 29.2, 48.1, 56.3, 68.4, 69.3, 82.2, 127.1, 128.2, 128.3, 136.4, 169.8; MS (EI) *m*/*z* % 266 (M^+).

Benzyl (*R*)-2-*O*-((*R*)-α-ethoxy-α-phenylacetyl)phenylacetate [(*R*)-14]: $[\alpha]_D = -71.10$ ($c = 0.052$; $CHCl_3$); ^{1}H NMR (250.17 MHz, MeCN-d_3) δ (ppm) 3.39 (s, 3H), 4.95 (s, 1H), 5.04 (d, $J = 12.50$ Hz, 1H), 5.08 (d, $J = 12.50$ Hz, 1H), 5.98 (s, 1H), 7.06−7.45 (m, 15H); ^{13}C NMR (75.42 MHz, MeCN-d_3) δ 56.7, 66.6, 74.6, 81.6, 127.1, 127.3, 127.6, 128.0, 128.2, 128.2, 128.4, 128.6, 129.2, 133.3, 135.2, 136.0, 167.9, 169.9; MS (EI) *m*/*z* % 390 (M^+).

Benzyl (*R*)-2-*O*-((*S*)-α-methoxy-α-phenylacetyl)phenylacetate [(*S*)-14]: $[\alpha]_D = -23.37$ ($c = 0.038$; $CHCl_3$); ^{1}H NMR (250.17 MHz, MeCN-d_3) δ (ppm) 3.33 (s, 3H), 4.95 (s, 1H), 5.13 (s, 2H), 5.95 (s, 1H), 6.84−7.26 (m, 15H); ^{13}C NMR (75.42 MHz, MeCN-d_3) δ 56.5, 66.6, 74.5, 81.6, 127.0, 127.0, 127.1, 127.5, 127.9, 128.1, 128.2, 128.4, 129.0, 133.1, 135.1, 135.9, 167.9, 169.8; MS (EI) *m*/*z* % 390 (M^+).

Benzyl (*S*)-2-*O*-((*R*)-α-methoxy-α-phenylacetyl)propionate [(*R*)-15]: $[\alpha]_D = -89.53$ ($c = 0.036$; $CHCl_3$); ^{1}H NMR (250.17 MHz, MeCN-d_3) δ (ppm) 1.39 (d, $J = 7.00$ Hz, 3H), 3.33 (s, 3H), 4.86 (s, 1H), 5.07 (dd, $J = 7.00$ Hz, 1H), 5.13 (s, 2H), 7.30−7,45 (m, 10H); ^{13}C NMR (75.42 MHz, MeCN-d_3) δ 15.8, 56.5, 66.4, 69.1, 81.7, 127.0, 127.80, 128.0, 128.3, 128.4, 135.5, 136.1, 169.9, 170.0; MS (EI) *m*/*z* % 328 (M^+).

Benzyl (*S*)-2-*O*-((*S*)-α-methoxy-α-phenylacetyl)propionate [(*S*)-15]: $[\alpha]_D = +17.76$ ($c = 0.037$; $CHCl_3$); ^{1}H NMR (250.17 MHz, MeCN-d_3) δ (ppm) 1.43 (d, $J = 7.00$ Hz, 3H), 3.36 (s, 3H), 4.86 (s, 1H), 5.05 (s, 2H), 5.11 (dd, $J = 7.00$ Hz, 1H), 7.23−7.44 (m, 10H); ^{13}C NMR (75.42 MHz, MeCN-d_3) δ 15.9, 56.5, 66.3, 69.0, 81.6, 127.1, 127.7, 127.9, 128.1, 128.2, 128.3, 135.4, 136.0, 169.7, 169.8; MS (EI) *m*/*z* % 328 (M^+)

Butyl (*S*)-2-*O*-((*R*)-α-methoxy-α-phenylacetyl)propionate [(*R*)-16]: $[\alpha]_D = -88.01$ ($c = 0.058$; $CHCl_3$); ^{1}H NMR (250.17 MHz, MeCN-d_3) δ (ppm) 0.90 (t, $J = 7.30$ Hz, 3H), 1.34 (m, 2H), 1.38 (d, $J = 7.07$, 3H), 1.55 (m, 2H), 3.38 (s, 3H), 4.09 (dt, $J = 3.50$, 6.50 Hz, 2H), 4.88 (s, 1H), 5.01 (dd, $J = 7.07$ Hz, 1H), 7.34−7.42 (m, 5H); ^{13}C NMR (75.42 MHz, MeCN-d_3) δ 12.6, 15.8, 18.4, 29.9, 56.5, 64.6, 69.1, 81.7, 127.0, 128.2, 128.4, 136.1, 169.9, 170.0; MS (EI) *m*/*z* % 294 (M^+).

Butyl (*S*)-2-*O*-((*S*)-α-methoxy-α-phenylacetyl)propionate [(*S*)-16]: $[\alpha]_D = +21.85$ ($c = 0.018$; $CHCl_3$); ^{1}H NMR (250.17 MHz, MeCN-d_3) δ (ppm) 0.87 (t, $J = 7.30$ Hz, 3H), 1.26 (m, 2H), 1.42 (d, $J = 7.07$, 3H), 1.45 (m, 2H), 3.39 (s, 3H), 4.01 (dt, $J = 3.50$, 6.50 Hz, 2H), 4.87 (s, 1H), 5.04 (dd, $J = 7.07$ Hz, 1H), 7.35−7.44 (m, 5H); ^{13}C NMR (75.42 MHz, MeCN-d_3) δ 12.6, 15.9, 18.3, 29.9, 56.5, 64.5, 69.0, 81.6, 127.1, 128.2, 128.3, 136.0, 169.8, 169.9; MS (EI) *m*/*z* % 294 (M^+).

Methyl 2-*O*-((*R*)-α-methoxy-α-phenylacetyl)-3,4-*O*-isopropylidene-L-threonate [(*R*)-17]: $[\alpha]_D = -22.05$ ($c = 0.039$; $CHCl_3$); ^{1}H NMR (250.17 MHz, MeCN-d_3) δ (ppm) 1.28 (s, 3H), 1.37 (s, 3H), 3.41 (s, 3H), 3.60 (s, 3H), 3.83 (dd, $J = 5.50$, 8.80 Hz, 1H), 4.06 (dd, $J = 6.80$, 8.80 Hz, 1H), 4.53 (m, 1H), 4.92 (s, 1H), 5.10 (d, $J = 3.8$ Hz, 1H), 7.06−7.46 (m, 5H); ^{13}C NMR (75.42 MHz, MeCN-d_3) δ 24.3, 25.1, 51.7, 56.6, 64.9, 72.1, 74.1, 81.8, 127.2, 128.1, 128.3, 128.4, 136.0, 167.3, 169.9; MS (EI) *m*/*z* % 338 (M^+).

Methyl 2-*O*-((*S*)-α-methoxy-α-phenylacetyl)-3,4-*O*-isopropylidene-L-threonate [(*S*)-17]: $[\alpha]_D = +62.84$ ($c = 0.025$; $CHCl_3$); ^{1}H NMR (250.17 MHz, MeCN-d_3) δ (ppm) 1.26 (s, 3H), 1.30 (s, 3H), 3.40 (s, 3H), 3.54 (dd, $J = 5.50$, 8.80 Hz, 1H), 3.69 (s, 3H), 3.96 (dd, $J = 7.00$, 8.80 Hz, 1H), 4.50 (m, 1H), 4.95 (s, 1H), 5.07 (d, $J = 3.80$ Hz, 1H), 7.05−7.48 (m, 5H); ^{13}C NMR (75.42 MHz, MeCN-d_3) δ 24.2, 25.0, 51.9, 56.6, 64.7, 71.9, 74.0, 81.7, 109.5, 127.0, 128.2, 128.4, 136.1, 167.4, 170.0; MS (EI) *m*/*z* % 338 (M^+).

Acknowledgment. This work was supported by grants from CICYT (PM98-0227, FEDER-CICYT 1FD97-2157) and from Xunta de Galicia (XUGA-PGIDT99-PXI20906B and XUGA-PGIDT99BIO20901). We thank "Centro de Supercomputación de Galicia" (CESGA) for time allocation for the calculations.

Supporting Information Available: The level of theory, specific program, basis set, matrixes, or Cartesian coordinates and computed total energies of optimized structures. This material is available free or charge via the Internet http://pubs.acs.org.

JO0256989

(31) Frisch, M. J.; Trucks, G. W.; Schlegel, H. B.; Scuseria, G. E.; Robb, M. A.; Cheeseman, J. R.; Zakrzewski, V. G.; Montgomery, J. A., Jr.; Stratmann, R. E.; Burant, J. C.; Dapprich, S.; Millam, J. M.; Daniels, A. D.; Kudin, K. N.; Strain, M. C.; Farkas, O.; Tomasi, J.; Barone, V.; Cossi, M.; Cammi, R.; Mennucci, B.; Pomelli, C.; Adamo, C.; Clifford, S.; Ochterski, J.; Petersson, G. A.; Ayala, P. Y.; Cui, Q.; Morokuma, K.; Malick, D. K.; Rabuck, A. D.; Raghavachari, K.; Foresman, J. B.; Cioslowski, J.; Ortiz, J. V.; Stefanov, B. B.; Liu, G.; Liashenko, A.; Piskorz, P.; Komaromi, I.; Gomperts, R.; Martin, R. L.; Fox, D. J.; Keith, T.; Al-Laham, M. A.; Peng, C. Y.; Nanayakkara, A.; Gonzalez, C.; Challacombe, M.; Gill, P. M. W.; Johnson, B. G.; Chen, W.; Wong, M. W.; Andres, J. L.; Head-Gordon, M.; Replogle, E. S.; Pople, J. A. *Gaussian 98*, revision A.7; Gaussian, Inc.: Pittsburgh, PA, 1998.